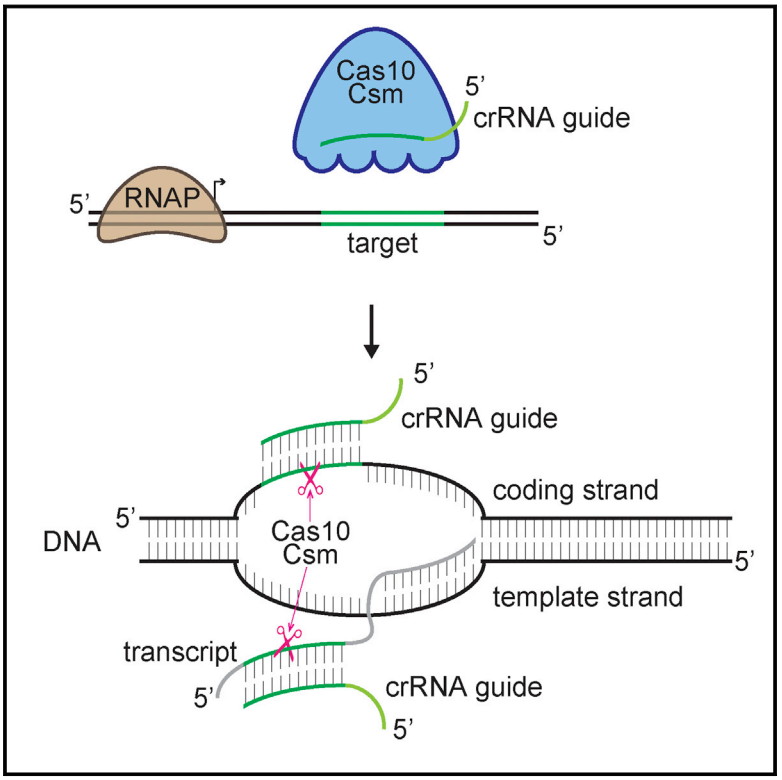
Article

Cell

Co-transcriptional DNA and RNA Cleavage during Type III CRISPR-Cas Immunity

Graphical Abstract



Highlights

- Type III CRISPR-Cas systems provide immunity when the target DNA is transcribed
- The type III Cas10-Csm complex performs co-transcriptional RNA-guided DNA cleavage
- The complex is also capable of RNA-guided RNA cleavage
- Both the target DNA and its transcript are subject to RNA-guided cleavage in vivo

Authors

Poulami Samai, Nora Pyenson, ...,
Asma Hatoum-Aslan,
Luciano A. Marraffini

Correspondence

marraffini@rockefeller.edu

In Brief

The type III-A CRISPR-Cas system is capable of RNA-guided DNA and RNA cleavage in vivo, revealing a highly versatile mechanism of CRISPR immunity that protects microorganisms against diverse DNA and RNA invaders.

Samai et al., 2015, Cell *161*, 1164–1174
May 21, 2015 ©2015 Elsevier Inc.
http://dx.doi.org/10.1016/j.cell.2015.04.027

CellPress

Cell

Article

Co-transcriptional DNA and RNA Cleavage during Type III CRISPR-Cas Immunity

Poulami Samai,[1] Nora Pyenson,[1] Wenyan Jiang,[1] Gregory W. Goldberg,[1] Asma Hatoum-Aslan,[1,2] and Luciano A. Marraffini[1,*]

[1]Laboratory of Bacteriology, The Rockefeller University, 1230 York Avenue, New York, NY 10065, USA

[2]Present address: Department of Biological Sciences, The University of Alabama, 300 Hackberry Lane, Tuscaloosa, AL 35487, USA

*Correspondence: marraffini@rockefeller.edu

http://dx.doi.org/10.1016/j.cell.2015.04.027

SUMMARY

Immune systems must recognize and destroy different pathogens that threaten the host. CRISPR-Cas immune systems protect prokaryotes from viral and plasmid infection utilizing small CRISPR RNAs that are complementary to the invader's genome and specify the targets of RNA-guided Cas nucleases. Type III CRISPR-Cas immunity requires target transcription, and whereas genetic studies demonstrated DNA targeting, in vitro data have shown crRNA-guided RNA cleavage. The molecular mechanism behind these disparate activities is not known. Here, we show that transcription across the targets of the *Staphylococcus epidermidis* type III-A CRISPR-Cas system results in the cleavage of the target DNA and its transcripts, mediated by independent active sites within the Cas10-Csm ribonucleoprotein effector complex. Immunity against plasmids and DNA viruses requires DNA, but not RNA, cleavage activity. Our studies reveal a highly versatile mechanism of CRISPR immunity that can defend microorganisms against diverse DNA and RNA invaders.

INTRODUCTION

CRISPR (clustered regularly interspaced short palindromic repeats) loci and their associated (*cas*) genes encode a prokaryotic adaptive immune system that provides protection against foreign nucleic acids such as viruses (Barrangou et al., 2007) and plasmids (Marraffini and Sontheimer, 2008). In this pathway, resistance is specified by sequences derived from past invaders that lie within the CRISPR loci interspersed between repeat elements, called spacers (Bolotin et al., 2005; Mojica et al., 2005; Pourcel et al., 2005). Repeats and spacers are transcribed into a long precursor crRNA (pre-crRNA). This precursor is processed into small interfering CRISPR RNAs (crRNAs) that together with Cas proteins assemble into a ribonucleoprotein (RNP) complex that uses the crRNA as a guide to locate and degrade the target nucleic acid (Brouns et al., 2008; van der Oost et al., 2014). Based on *cas* gene content, CRISPR-Cas systems have been categorized into three major types (I–III) (Makarova et al., 2011b). In type III systems, pre-crRNA processing is carried out by Cas6, a repeat-specific endoribonuclease (Carte et al., 2008; Hatoum-Aslan et al., 2014). Cas6 cleavage at repeat sequences generates crRNAs containing a full spacer sequence flanked by an 8-nt repeat sequence at the 5′ end (the crRNA "tag") and the rest of the repeat at the 3′ (Carte et al., 2008; Marraffini and Sontheimer, 2008). A yet-uncharacterized nuclease is involved in further trimming of the 3′ end repeat sequence to produce a heterogeneous population of mature crRNA species that differ by 6 nt in length (Hatoum-Aslan et al., 2011, 2013).

Type III CRISPR-Cas systems are further classified into III-A and III-B subtypes. Both systems harbor the type III-defining *cas10* gene, but they are distinguished by the content of accessory genes: *csm* for III-A systems and *cmr* for type III-B (Makarova et al., 2011b). The crRNA-guided targeting of nucleic acids by type III-A CRISPR-Cas systems is highly sophisticated. In vivo, targeting requires the lack of homology between the crRNA tag and the target 5′ flanking sequence (Marraffini and Sontheimer, 2010). This requirement is thought to distinguish between bona fide targets on invading nucleic acids from the CRISPR array itself, where the presence of repeat sequences will lead to full homology with the crRNA tag and prevent autoimmunity. In addition, transcription across the target is required for targeting in vivo (Goldberg et al., 2014). The nature of the target nucleic acid has been controversial. In vivo genetic assays demonstrated DNA targeting for the type III-A system of *Staphylococcus epidermidis* (Goldberg et al., 2014; Hatoum-Aslan et al., 2014; Marraffini and Sontheimer, 2008) but RNA targeting for the *Streptococcus thermophilus* system (Tamulaitis et al., 2014). Recently, crRNA-guided RNA targeting has been shown in vitro (Staals et al., 2014; Tamulaitis et al., 2014); however, direct demonstration of DNA cleavage has not been provided yet.

Here, we performed in vivo and in vitro experiments with the type III-A CRISPR-Cas system of *S. epidermidis*, which demonstrate dual crRNA-guided cleavage of the target DNA and its transcripts. We show that purified Cas10-Csm complexes cleave double-stranded DNA targets. The reaction absolutely requires transcription across the target, and it is inhibited by the presence of homology between the crRNA tag and the 5′ target flanking sequence. The same complex is also capable of crRNA-guided RNA cleavage in vitro, and this reaction is not prevented by crRNA tag homology. In vivo, type III-A targeting of a plasmid shows degradation of the DNA upon induction of transcription

CrossMark

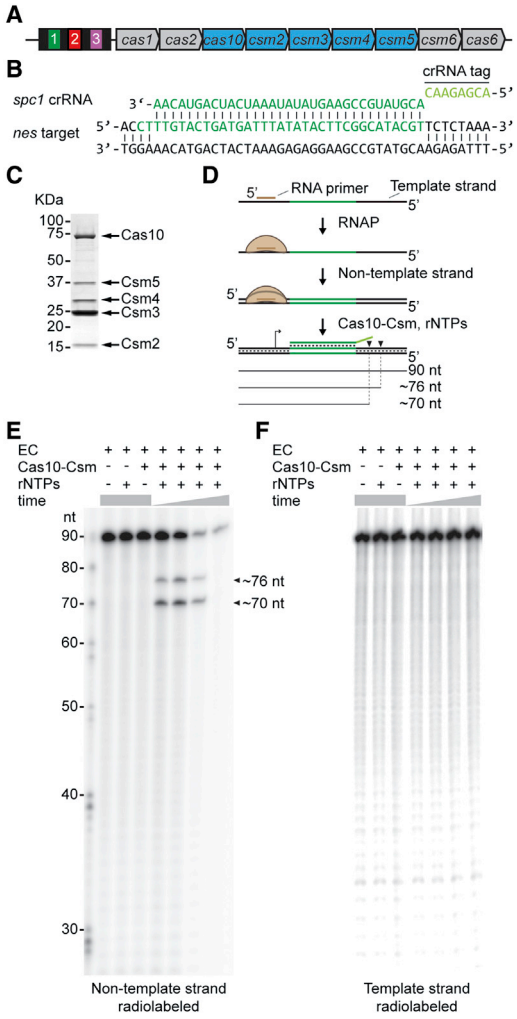


Figure 1. crRNA-Guided Co-transcriptional DNA Cleavage by the *S. epidermidis* Cas10-Csm Complex

(A) *S. epidermidis* RP62a carries a CRISPR-Cas locus that harbors four repeats (black boxes), three spacers (colored boxes), and nine *cas/csm* genes, five of which (highlighted in blue) encode for the Cas10-Csm ribonucleoprotein complex.

(B) The first spacer sequence (*spc1*) generates a mature crRNA that targets a complementary sequence in the *nickase* gene (*nes*) present in most staphylococcal conjugative plasmids (green). The most abundant mature crRNA species contains 33 nt of spacer sequence as well as 8 nt of repeat sequences at its 5′ end, known as the crRNA tag (light green).

(C) SDS-PAGE of the Cas10-Csm complex purified from *E. coli*.

(D) Schematic of the co-transcriptional DNA cleavage assay of a dsDNA substrate containing the *nes* target. Arrowheads indicate the approximate cleavage site detected in (E).

(E and F) Denaturing PAGE and autoradiography of the products of two co-transcriptional dsDNA cleavage assays differing in the location of the radioactive label: (E) non-template strand; (F) template strand. Cleavage products were collected at 30, 60, 90, and 120 min. Reactions in which each of the components of the assay were omitted in a 120-min assay are shown as controls.

across the target, as well as a precise cut of the target transcript. We also show that DNA and RNA targeting are independent events. Whereas DNA targeting requires an intact Cas10 palm polymerase domain, RNA targeting requires a nucleolytic active site in Csm3, both in vitro and in vivo. Mutations that affect DNA cleavage do not affect RNA cleavage and vice versa. Finally, in vivo experiments show that DNA, but not RNA, cleavage is required for immunity against plasmids and DNA viruses. These results consolidate all the different mechanistic observations of type III-A targeting into a single model and uncover a highly elaborate targeting strategy distinct from the type I and type II CRISPR-Cas systems studied so far (Barrangou and Marraffini, 2014).

RESULTS

crRNA-Guided DNA Cleavage by the Cas10-Csm Complex Requires Target Transcription

Whereas genetic evidence demonstrated DNA targeting for the *S. epidermidis* type III-A CRISPR-Cas system (Goldberg et al., 2014; Hatoum-Aslan et al., 2014; Marraffini and Sontheimer, 2008), direct evidence of DNA cleavage has been elusive. We previously showed that the *S. epidermidis* CRISPR-Cas locus (Figure 1A) encodes for a ribonucleoprotein complex composed of Cas10, Csm2, Csm3, Csm4, Csm5, and the crRNA guide, known as the Cas10-Csm complex (Hatoum-Aslan et al., 2013, 2014). One of the crRNAs (encoded by the first spacer, *spc1*) matches a region of the *nickase* gene present in most staphylococcal conjugative plasmids (Marraffini and Sontheimer, 2008); this region was selected as the target for our in vivo and in vitro studies (Figure 1B). We expressed these proteins in *Escherichia coli* to purify the complex to homogeneity (Figure 1C). The complex was co-expressed with the repeat-spacer array, and therefore it is loaded with the mature crRNA species that differ by increments of 6 nt (Figure S1A). As observed for other type III-A CRISPR-Cas systems (Staals et al., 2014; Tamulaitis et al., 2014), the Cas10-Csm complex was incapable of cleaving a complementary single-stranded DNA (ssDNA) or double-stranded DNA (dsDNA) oligonucleotide substrates in different assay conditions (Figures S1B and S1C). Recently, we reported that transcription of the target sequence is required for type III-A CRISPR immunity (Goldberg et al., 2014). In order to test whether target transcription facilitates DNA cleavage, we used an oligonucleotide-based RNAP transcription system, where stepwise assembly of purified RNA and DNA oligonucleotides and *E. coli* core RNA polymerase can reconstitute fully functional RNAP elongation complexes (Sidorenkov et al., 1998). In this assay, each oligonucleotide (the RNA primer, the template strand or the non-template strand) can be radioactively labeled prior to assembly to follow their fate in the reaction. The DNA oligonucleotides were complementary to each other and contained the *nes* target (35 nt complementary to the *spc1* crRNA) and its flanking sequences (24 nt on each side). The elongation complex is assembled in the presence of transcription buffer containing Mg^{2+} by the annealing of an RNA primer to the template strand, followed by the addition of RNAP and the annealing of the non-template strand (Figure 1D). Assembled elongation complexes were incubated with purified Cas10-Csm, and transcription was started by supplementing rNTPs. Extension of 5′-radiolabeled RNA primers confirmed transcription elongation (Figure S1D). We labeled each strand of the

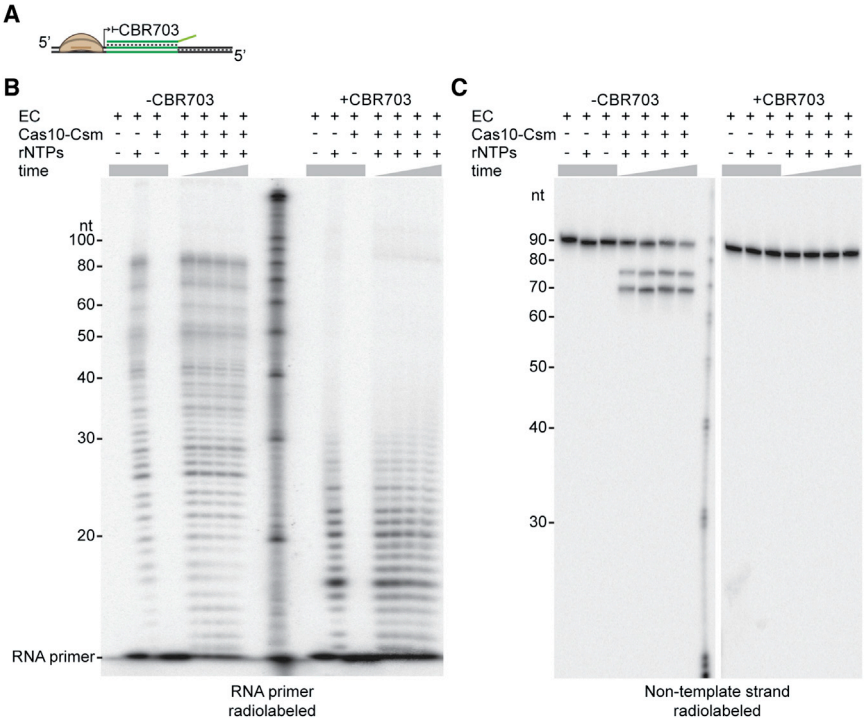


Figure 2. RNAP Elongation Is Required for Cas10-Csm Target Cleavage

(A) The small molecule CBR703 inhibits RNAP elongation and was tested in our DNA cleavage assay to corroborate the transcription requirement for cleavage.

(B) CBR703 inhibits transcription elongation. Using a radiolabeled RNA primer, we measured transcription elongation in different conditions in the presence (1 μM) or absence of CBR703. Extension products were collected at 30, 60, 90, and 120 min. Reactions in which each of the components of the assay was omitted in a 120-min assay are shown as controls.

(C) In vitro DNA cleavage assay using a radiolabeled non-template strand (as in Figure 1E) in the presence (1 μM) or absence of CBR703. Reaction products were collected at 30, 60, 90, and 120 min. Reactions in which each of the components of the assay was omitted in a 120-min assay are shown as controls.

substrate in different experiments and analyzed the products of the reaction by denaturing PAGE and autoradiography. We detected cleavage of the non-template strand at two defined sites, only after the start of transcription by the addition of rNTPs (compare lanes 3 and 4–7, Figure 1E). Interestingly, an estimation of the cleavage sites based on the size of the product indicates that it occurred on the 3′ flanking side of the target, not within the region with complementary to the crRNA (Figure 1D). Further DNA degradation to the nucleotide level was observed with longer incubation times (Figure 1E). The template strand, in contrast, was neither cleaved nor degraded (Figure 1F). To unequivocally demonstrate a transcription requirement for DNA cleavage, we used an RNAP elongation inhibitor, CBR703 (Artsimovitch et al., 2003). This small molecule inhibitor prevents nucleotide addition during transcription and therefore it should impair DNA cleavage by the Cas10-Csm complex (Figure 2A). First we corroborated that the addition of CBR703 prevents efficient transcription elongation in our assay, by radiolabeling the RNA primer (Figure 2B). When the same assay was performed using a radiolabeled non-template strand, the inhibition of transcription elongation with CBR703 prevented DNA cleavage (Figure 2C). Altogether these results reveal the molecular mechanism of type III-A DNA targeting: transcription-dependent DNA cleavage of the non-template strand.

Two previous genetic observations revealed an unexpected targeting mechanism for type III-A systems. First, only crRNAs complementary to the non-template strand provide efficient immunity (Goldberg et al., 2014) (Figures S2A and S2B). Second, the prevention of autoimmunity in type III-A systems, i.e., the *spc1* crRNA-guided targeting of *spc1* DNA in the CRISPR array, requires homology between the crRNA tag and the repeat sequences that flank the 3′ end of the spacer DNA (of the targeted strand, complementary to the crRNA spacer sequence) (Marraffini and Sontheimer, 2010) (Figure S2C). Presumably this is achieved by the pairing between these sequences. The development of an in vitro DNA cleavage assay allowed us to test whether the lack of immunity observed in these two genetic experiments reflects an abrogation of target DNA cleavage by the Cas10-Csm complex. To test for DNA cleavage mediated by a crRNA complementary to the template strand, we used an RNA primer that anneals to the top strand of our dsDNA substrate to assemble the elongation complex (Figure 3A). Incubation with the Cas10-Csm complex in identical conditions to those that led to cleavage of the non-template strand produced no cleavage of either strand (Figure 3B), even in the presence of target transcription (Figure S1D). To test for DNA cleavage in the anti-autoimmunity scenario, we modified the target to introduce the corresponding repeat sequences at the 3′ flank of the *spc1* crRNA complementarity region (Figure 3C). We then assembled the elongation complex and tested for cleavage of each DNA strand. We did not detect any cleavage or degradation, regardless of target transcription (Figure 3D). This result indicates that, in addition to target transcription, DNA cleavage requires mismatches between the crRNA tag and the 3′ flanking region of the target, thus providing the molecular basis for the prevention of autoimmunity, a central feature of all immune systems.

crRNA-Guided RNA Cleavage by the Cas10-Csm Complex

Recently, it has been reported that type IIIA in *Streptococcus thermophilus and Thermus thermophilus* can cleave ssRNA targets (Staals et al., 2014; Tamulaitis et al., 2014), a function that allows protection against RNA viruses (Tamulaitis et al., 2014). In both of these systems, the Cas10-Csm complex cleaves

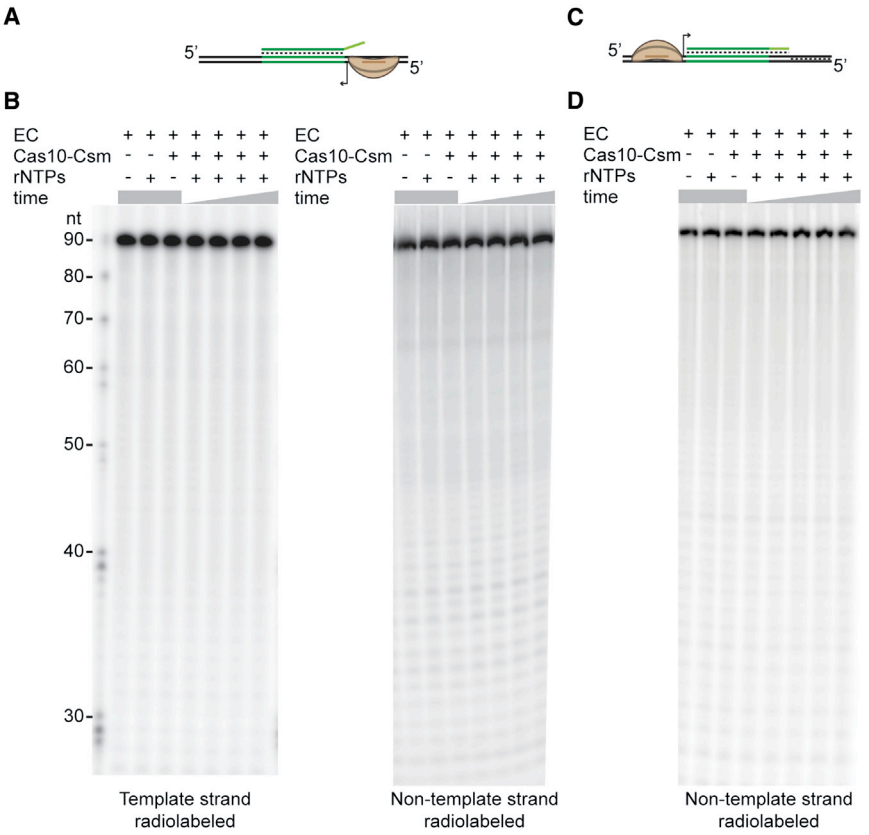


Figure 3. In Vitro Cleavage Reflects In Vivo Targeting

(A) Schematic of the substrate used to test for DNA cleavage in conditions where the crRNA matches the template strand.

(B) In vitro DNA cleavage assay of the substrate shown in (A), with the radiolabel either in the template (left autoradiography) or non-template (right) strand. Reaction products were collected at 30, 60, 90, and 120 min. Reactions in which each of the components of the assay was omitted in a 120-min assay are shown as controls.

(C) Schematic of the "anti-tag" substrate in which the flanking sequence downstream on the *nes* target matches the 5′ crRNA tag (light green), generating a full match between the crRNA and the DNA target.

(D) In vitro DNA cleavage assay of the substrate shown in (C), with the non-template strand radiolabeled. Reaction products were collected at 30, 60, 90, 120, and 180 min. Reactions in which each of the components of the assay was omitted in a 120-min assay are shown as controls.

RNA at multiple sites at 6-nt intervals. We also investigated the ribonuclease activity of the *S. epidermidis* complex. A 55-nt, 5′-radiolabeled ssRNA substrate complementary to *spc1* crRNA (Figure 4A) was incubated with the Cas10-Csm complex in a buffer containing Mg^{2+}, and the reaction was subjected to denaturing gel separation and autoradiography. We observed sequence specific endoribonuclease activity against the ssRNA substrate complementary to *spc1* crRNA, with multiple cleavage products showing the reported 6-nt periodicity (Figure 4C; Figures S3A and S3B). No activity was observed with a 55-nt scrambled, control RNA substrate (Figures S3C and S3D). A conserved aspartate residue in Csm3 (D32 in the *S. epidermidis* homolog) was identified to be the active site residue responsible for the endoribonuclease activity in the *S. thermophilus* and *T. thermophilus* complexes (Staals et al., 2014; Tamulaitis et al., 2014). We made the corresponding alanine substitution, D32A, purified the Cas10-Csm(Csm3^{D32A}) complex, and tested its activity against ssRNA substrates. The Csm3 D32A mutant impaired RNA cleavage without affecting complex assembly or crRNA maturation (Figures 4D and S1A), consistent with a requirement for this conserved aspartate in the catalysis of RNA cleavage. Finally, to interrogate the importance of base-pairing between the crRNA tag and the 3′-flanking sequence of the target, we used an ssRNA substrate (anti-tag *nes* ssRNA substrate, Figure 4B) with a sequence complementary to the tag. PAGE analysis of the reaction products revealed that base-pairing between the 8-nt crRNA tag and the 3′-flanking sequence of the target had no effect on the ssRNA cleavage pattern (Figure 4E). Collectively, the data in Figures 4 and S3 corroborate previous reports of crRNA-guided RNA cleavage by type III-A CRISPR-Cas systems. More important, together with our demonstration of DNA cleavage these findings reveal that type III-A immunity is capable of both RNA and DNA targeting.

crRNA-Guided RNA and DNA Cleavage Are Independent Activities within the Cas10-Csm Complex

Combined with the crRNA-guided RNA cleavage, the transcription requirement for type III-A CRISPR-Cas immunity and crRNA-guided DNA cleavage opens the possibility of a mechanistic link between these two activities. For example, the RNA cleavage of the target's transcript could be required for DNA cleavage. However, because experiments with substrates containing a 3′ flanking sequence capable of pairing with the crRNA tag had opposite outcomes, i.e., DNA but not RNA cleavage was affected (see above), our results suggest that these are independent cleavage activities. To test this, we evaluated the DNA cleavage activity of the Cas10-Csm(Csm3^{D32A}) complex, incapable of RNA cleavage. The mutant generated a similar DNA cleavage pattern of the non-template strand to the wild-type complex (Figure 5A, compare to Figure 1E). This demonstrates that the Csm3 active site is not responsible for DNA cleavage and that DNA targeting occurs independently of RNA cleavage.

Cas10 is the largest subunit of the type III-A effector complex and contains a degenerate GGDEF motif (GGDD), resembling the palm polymerase domain of DNA/RNA polymerases and nucleotidyl cyclases (Anantharaman et al., 2010; Makarova et al., 2011a). Previously, we reported that mutations in the palm domain of *cas10* (*cas10*^{G584A,G585A,D586A,D587A}, here abbreviated

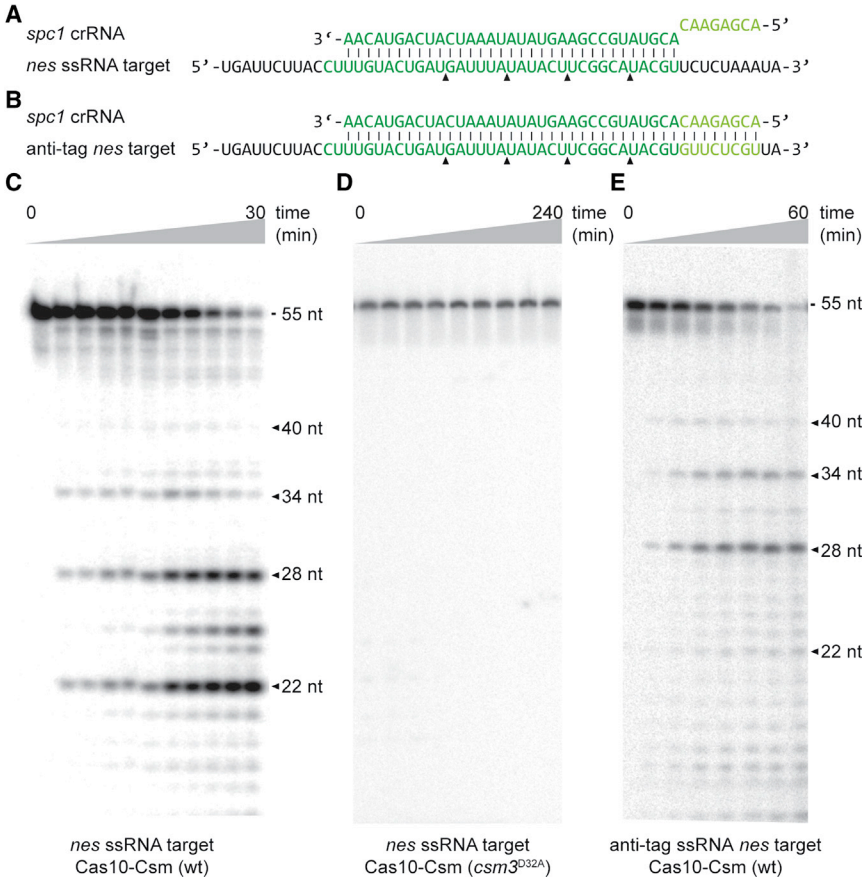


Figure 4. crRNA-Guided RNA Cleavage by the *S. epidermidis* Cas10-Csm Complex

(A) Base-pair interaction between the *nes* crRNA and the 55-nt ssRNA target. Arrowheads showed the cleavage sites detected in (C).

(B) "Anti-tag" ssRNA substrate used to evaluate the effect of a full match between the crRNA guide and the ssRNA substrate. Arrowheads showed the cleavage sites detected in (E).

(C) In vitro ssRNA cleavage assay of the radiolabeled substrate shown in (A). Reaction products were collected at 0, 1, 2, 3, 4, 5, 7.5, 10, 15, 20, and 30 min, separated by denaturing PAGE and visualized by gel autoradiography.

(D) Same assay as in (C), using the mutant Cas10-Csm(Csm3^{D32A}) complex. Incubation times are 0, 5, 10, 20, 30, 60, 120, 180, and 240 min.

(E) Cleavage of the "anti-tag" ssRNA substrate shown in (B); incubation times: 0, 5, 10, 15, 30, and 60 min.

cas10^{palm}) are required for type III-A immunity against staphylococcal plasmids (Hatoum-Aslan et al., 2014). The mutant did not show defects in either crRNA maturation or Cas10-Csm complex formation, suggesting that the palm polymerase domain could play a catalytic role in plasmid targeting (Hatoum-Aslan et al., 2014). To investigate this, we purified a Cas10-Csm complex with alanine substitutions of the conserved aspartate residues (Cas10^{D586A,D587A}-Csm) and tested it for RNA or DNA nuclease activity. Whereas the mutant complex cleaved the ssRNA substrate with a similar pattern as the wild-type complex (Figure 5B, compare to Figure 4C), it was defective in co-transcriptional DNA cleavage (Figure 5C). These results demonstrate that the palm polymerase domain of Cas10 plays an essential role in DNA cleavage, with its two conserved aspartate residues most likely involved in catalysis. Taken together, these data indicate that crRNA-guided DNA cleavage activity of type III-A CRISPR-Cas systems is independent from the crRNA-guided RNA cleavage, catalyzed by two different active sites within the Cas10-Csm complex.

Dual crRNA-Guided Cleavage of a DNA Target and Its Transcripts during Type III-A CRISPR Immunity

Although the DNA and RNA cleavage activities of the Cas10-Csm complex are independent, our data clearly indicate that type III-A CRISPR-Cas systems can cleave both DNA and RNA molecules. Moreover, the crRNAs that confer immunity and mediate DNA cleavage (which match the non-template, not the template, DNA strand) are also complementary to, and can guide cleavage of, the target transcript (Figure 6A). It is therefore possible that type III-A CRISPR immunity results in the cleavage of both the target DNA and its transcripts. To test this, we utilized an inducible immunity assay in vivo. In this assay, cells harbor a plasmid with the *nes* target under the control of a tetracycline-inducible promoter, the pTarget plasmid. To study the effect of a match between the 3′ flanking target sequence and the crRNA tag, we generated a mutant version of pTarget with mutations upstream of the *nes* target that introduce this match (the pTarget$^{anti\text{-}tag}$ plasmid, Figure S2C). Finally, the third strain tested contained pE194, an empty vector control. These cells are then transformed with a second plasmid encoding the type III-A CRISPR-Cas system (wild-type or the mutant variants Δ*spc1*, *cas10*^{palm}, or *csm3*^{D32A}), the pCRISPR plasmid. Previous studies confirmed the heterologous expression of the Cas10-Csm complex from this plasmid (Hatoum-Aslan et al., 2013). In the absence of the inducer, anhydrotetracycline (aTc), there is no target transcription, and therefore there should be no immunity against pTarget and its derivatives. Isolated transformants can be treated with aTc to induce CRISPR immunity and follow the fate of the target DNA and its transcripts (Figure 6B). First we performed transformations and seeded plates with or without aTc to measure CRISPR immunity. In the presence of aTc (Figure 6C), cells harboring pTarget and the control pE194 plasmids had similarly high efficiency of transformation for pCRISPR(Δ*spc1*), which does not express the *spc1* crRNA guide, and for the DNA cleavage-deficient pCRISPR(*cas10*^{palm}). The efficiency of transformation of cells containing the pTarget$^{anti\text{-}tag}$ with the wild-type pCRISPR was also high. In contrast, transformation of the wild-type and *csm3*^{D32A} pCRISPR plasmids was greatly diminished in recipients harboring pTarget

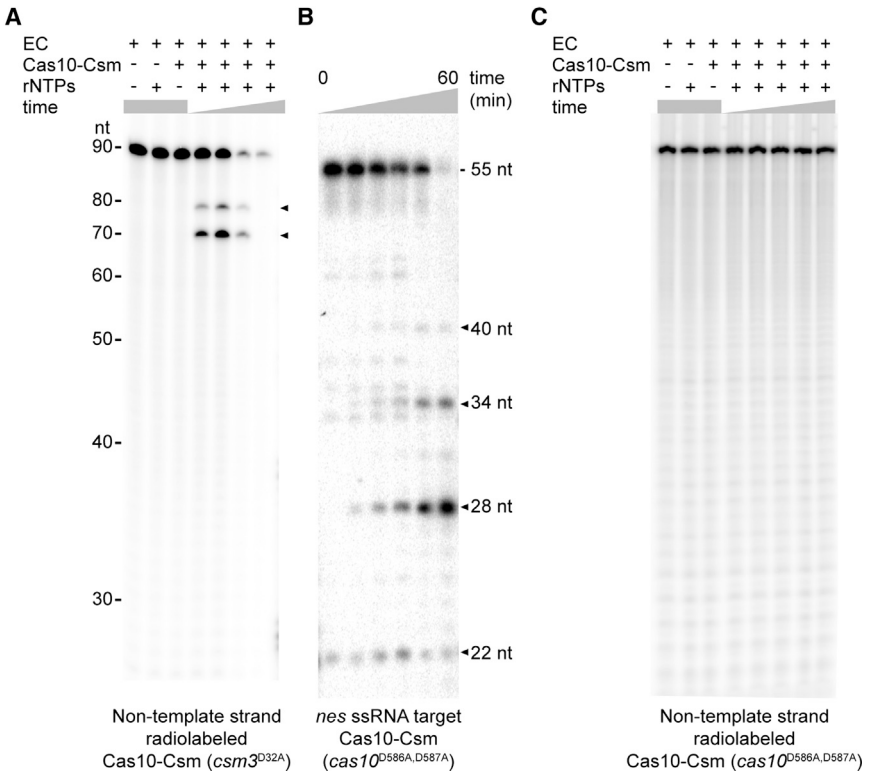


Figure 5. The DNA and RNA Cleavage Activities of the Cas10-Csm Complex Are Independent

(A) Same DNA cleavage assay shown in Figure 1E using the Cas10-Csm(Csm3^{D32A}) complex.

(B) Same ssRNA cleavage assay shown in Figure 3C using the Cas10^{D586A,D587A}-Csm complex; incubation times: 0, 5, 10, 15, 30, and 60 min.

(C) Same DNA cleavage assay shown in Figure 1E using the Cas10^{D586A,D587A}-Csm complex. An extra time point was taken at 180 min.

but not pE194 or pTarget$^{anti\text{-}tag}$. Collectively, these results demonstrate that cleavage of the DNA target, but not its transcript, is required for CRISPR immunity against plasmids. As expected, when we plated in the absence of the inducer (Figure 6D), we measured a high efficiency of transformation for all plasmids. An exception was the transformation of the pCRISPR(*csm3*^{D32A}) plasmid into cells harboring pTarget. In this case, we obtained a decrease in the number of transformants of approximately three orders of magnitude, with all of the colonies tested resulting in "escaper" mutants that either lacked the target or harbored rearranged pCRISPR(*csm3*^{D32A}) plasmids (not shown). We do not understand this gain-of-function phenotype, but we speculate that there is an increase of DNA targeting in the absence of RNA targeting, which is highly susceptible to leaky expression of the *nes* target in the absence of aTc. This could be due to the presence of more Cas10-Csm complexes available for DNA targeting in the absence of RNA targeting in this mutant. The reduction in transformation efficiency was not observed when pCRISPR(*csm3*^{D32A}) was transformed into pE194-containing cells or when a second, wild-type copy of *csm3* was added into the assay (data not shown).

Staphylococci containing both the target and CRISPR plasmids (pCRISPR/pTarget, pCRISPR/pTarget$^{anti\text{-}tag}$, pCRISPR(Δ*spc1*)/pTarget and pCRISPR(*cas10*^{palm})/pTarget) obtained after transformation in the absence of aTc were further analyzed to detect DNA and/or RNA cleavage upon induction of target transcription. Transformants were grown in liquid to an OD_{600} ~0.5 before the addition of aTc. Plasmid DNA and total RNA were extracted from cells collected at different times after transcription induction. The integrity of the plasmid DNA was observed by agarose gel electrophoresis followed by ethidium bromide staining before and after addition of aTc (Figure 6E). The different versions of pCRISPR are not targeted and therefore serve as a loading control for each lane. While the pTarget was completely degraded in the presence of a wild-type pCRISPR, it was detected in cells containing the *cas10*^{palm} mutation, albeit at lower levels than in cells lacking the *spc1* crRNA. pTarget$^{anti\text{-}tag}$ was also intact in the presence of the wild-type pCRISPR. Analysis of pTarget degradation over time revealed the disappearance of the supercoiled plasmid (Figure 6F). RNA cleavage was followed by primer extension of total RNA with an oligonucleotide priming downstream of the *nes* target transcript (Figure 6G). Extension of the full *nes* transcript (171 nt) was detected in cells lacking the *spc1* crRNA guide, but cleavage products were observed for wild-type and *cas10*^{palm} CRISPR-Cas systems, with cleavage site within the *nes* target (Figure 6H). Although in vitro we detected multiple cleavage sites, only the nearest downstream cleavage site is detected in vivo, most likely due to the impossibility of extending beyond the cut RNA. Cleavage of the anti-tag *nes* transcript was detected, although at a position that maps downstream of the target (see Discussion). Altogether, these results demonstrate that cleavage of the target DNA, but not its transcripts, is required for type III-A CRISPR-Cas immunity against plasmids. More importantly, the data show that these systems are capable of co-transcriptional DNA targeting resulting in the cleavage of both the target DNA and its transcripts.

As opposed to our plasmid experiments, in which the target transcript is not essential for plasmid replication, most viral transcripts are essential for viral propagation. Therefore, we investigated whether the dual DNA and RNA cleavage of the viral target DNA and its transcripts is important for anti-phage immunity. We tested the protection of staphylococci harboring different mutations in the type III-A CRISPR-Cas locus against infection by the dsDNA bacteriophage ΦNM1γ6 (Goldberg et al., 2014). We targeted the head protein gene *gp43* (Figure 7A) and measured cell survival (Figure 7B). As shown before (Goldberg et al., 2014), the wild-type CRISPR-Cas system provided strong immunity. In contrast, cells containing the *cas10*^{palm} gene succumbed to

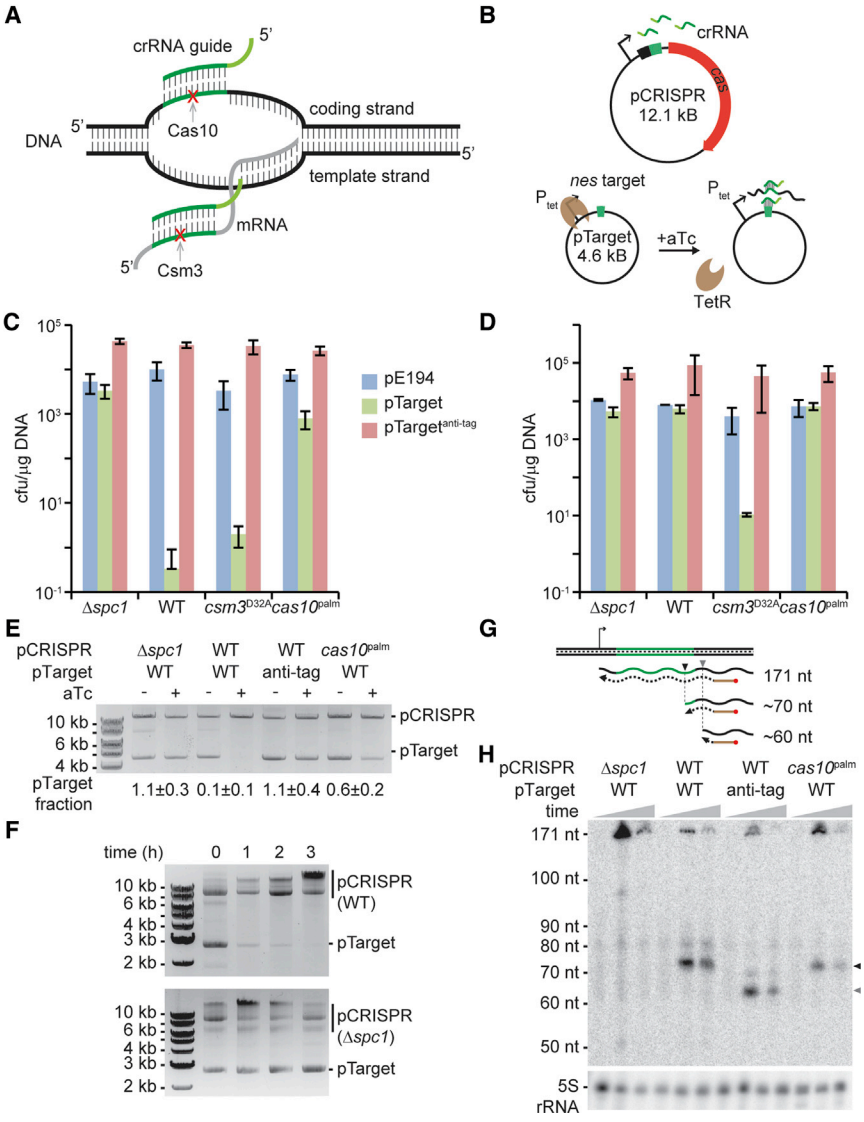


Figure 6. crRNA-Guided Co-transcriptional Cleavage of Plasmid DNA and Its Transcripts during Type III-A CRISPR-Cas Immunity

(A) Schematic of the dual crRNA-guided DNA and transcript RNA cleavage (red cross). Target sequences are shown in green; the nuclease responsible for the cleavage of each nucleic acid is also indicated.

(B) Inducible anti-plasmid CRISPR immunity assay. Staphylococci are transformed with two plasmids: pCRISPR carrying the type III-A CRISPR-Cas system of *S. epidermidis* and pTarget harboring the *nes* target under the control of the tetracycline-inducible promoter P_{tet}. In the absence of the anhydro-tetracycine inducer (aTc), the tetracycline repressor (TetR) prevents *nes* transcription and therefore CRISPR immunity against pTarget. Addition of aTc triggers immunity, allowing following the fate of pTarget and its transcripts over time.

(C) Transformation efficiencies of different pCRISPR plasmids (wild-type or the mutant variants Δ*spc1*, *cas10*^{palm} or *csm3*^{D32A}) into staphylococci harboring different target plasmids (pE194, pTarget, and pTarget$^{anti\text{-}tag}$). Efficiency is calculated as the ratio of colony-forming units (cfu) per microgram of plasmid DNA transformed (mean ± SD of three replicas). Colonies were enumerated in plates containing chloramphenicol and erythromycin for the selection of pCRISPR and pTarget, respectively, and aTc.

(D) Same as (C), but without supplementing plates with aTc.

(E) pTarget transformants obtained in (D) were cultured in liquid media supplemented with chloramphenicol but without erythromycin. Cells were collected at the beginning of the exponential growth, before aTc was added (–), and after 10 hr of growth in the presence of the inducer (+). Plasmid DNA was extracted, digested with XhoI, separated by agarose gel electrophoresis and stained with ethidium bromide. The fraction of pTarget remaining after targeting relative to the pCRISPR control is shown at the bottom of the gel (mean ± SD of three replicas).

(F) Analysis of pTarget plasmid DNA at different times during type III-A CRISPR-Cas immunity (wild-type pCRISPR) or a non-targeting control (Δ*spc1* pCRISPR), without XhoI digestion.

(G) Schematic of a primer extension assay designed to detect *nes* transcript cleavage during type III-A CRISPR-Cas immunity. A 5′-radiolabeled (red dot) primer (brown line) is used to initiate reverse transcription of the *nes* transcript, generating a 171-nt extension product in the absence of RNA cleavage, measured from the priming site to the +1 transcription start determined by the P_{tet} promoter (arrow). The cleavage sites inferred from the results shown in (H) are indicated, approximately 70 and 60 nt from the priming site (black and gray arrowheads, respectively).

(H) Primer extension analysis of the *nes* transcripts after addition of aTc in different targeting conditions. Times assayed: 0, 10, and 60 min. Arrowheads indicated the extension of the cleavage products.

phage infection. The CRISPR-Cas systems containing the *csm3*^{D32A} mutation, which cannot cleave the target's transcript, provided similar immunity to the wild-type system, almost indistinguishable from the protection conferred by the type II-A CRISPR-Cas system of *Streptococcus pyogenes* (incapable of RNA cleavage) targeting the same viral region (Figure 7). These results support the hypothesis that DNA and RNA cleavage activities are independent and that the crRNA-guided RNA cleavage of the Cas10-Csm complex is not required for defense against dsDNA viruses, at least in the conditions tested.

DISCUSSION

Recently, we showed that the immunity provided by type III-A CRISPR-Cas systems demands target transcription and that only crRNAs complementary to the non-template (coding) strand provide effective immunity (Goldberg et al., 2014). Previously, it was shown that self versus non-self discrimination in these systems relies upon the differential base-pairing of the crRNA tag to the target flanking sequences (Marraffini and Sontheimer, 2010), rather than on the presence of the protospacer-adjacent motif

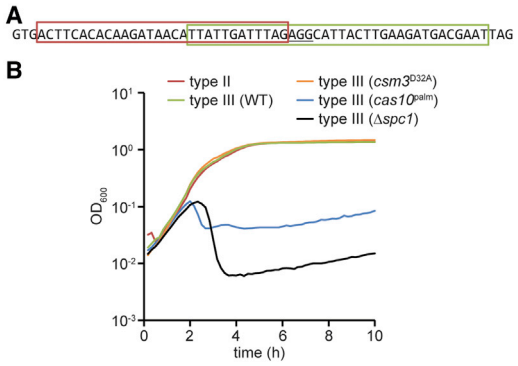


Figure 7. Immunity against dsDNA Viruses Requires the DNA, but Not the RNA, Cleavage Activity of the Cas10-Csm Complex

(A) Sequence of the *gp43* gene of the ϕNM1γ6 staphylococcal dsDNA phage (22,390–22,449 bp) targeted by both type III-A (green box) and type II-A (red box) CRISPR-Cas systems.

(B) Staphylococci harboring different CRISPR-Cas systems targeting the *gp43* gene as shown in (A) were grown in liquid media and infected with ϕNM1γ6 phage (at 0 hr). Optical density was measured for the following 10 hr to monitor cell survival due to CRISPR immunity against the phage.

(PAM) of type I and II CRISPR-Cas targets (Bolotin et al., 2005; Deveau et al., 2008; Mojica et al., 2009; Semenova et al., 2011). Here, we reconstituted DNA cleavage by the type III-A Cas10-Csm ribonucleoprotein complex in vitro, demonstrating that (1) cleavage requires the transcription of the target DNA, (2) only crRNA guides complementary to the non-template strand can direct cleavage, (3) pairing between the crRNA tag and the 3′ flanking sequence of the target prevents cleavage, and (4) the Cas10 palm polymerase domain is involved. Thus, our biochemical results provide the molecular mechanism for the most basic aspects of type III-A CRISPR-Cas immunity against DNA mobile genetic elements. Intriguingly, the DNA cleavage site lies outside the target sequence complementary to the crRNA, mapping to the 3′ flanking side of the target. Perhaps the Cas10-Csm complex probes the base-pairing nature between the 8-nt crRNA-tag and the 3′-flanking sequence of the target, to distinguish the CRISPR array from bona fide targets and avoid cleavage of the former. Our previous genetic data suggested that DNA targeting requires transcription in *cis* (Goldberg et al., 2014). We speculate that co-transcriptional DNA cleavage may result from either the separation of both DNA strands or negative DNA supercoiling, both facilitated by translocation of the transcriptional machinery along DNA. Accumulation of negative supercoiling has been determined a requisite for DNA cleavage by the type I-E CRISPR-Cas system (Westra et al., 2012). Purification followed by mass spectrometry of the Cas10-Csm complex from staphylococci showed the absence of co-purifying RNAP subunits (Hatoum-Aslan et al., 2013, 2014), suggesting the absence of a detectable interaction between both complexes. Our cleavage experiments indicate that only the non-template strand is cleaved, raising the question of how a single-strand break in the phage DNA can result in strong immunity. Experiments using a nickase version of the dsDNA nuclease EcoRI have shown that the introduction of chromosomal DNA nicks is toxic to the cell, and even lethal in the absence of the homologous recombination repair pathway (Heitman et al., 1999). Presumably, the passage of a replication fork through the ssDNA break creates more severe DNA lesions that cannot be repaired by simple ligation and that induce the SOS repair system. We believe that a similar scenario can apply to the Cas10-Csm nickase activity on phage DNA targets: it could lead to severe DNA damage that is not repaired efficiently, preventing viral replication. This also could be the case for type I-E systems, where the Cas3-Cascade complex has been reported to introduce single-strand breaks on its DNA targets (Westra et al., 2012). In vivo, following the target plasmid after induction of CRISPR targeting, we cannot detect nicked nor linearized DNA. Instead, we observe the disappearance of the supercoiled form of the plasmid. We hypothesize that in vivo the nicked plasmid species is rapidly degraded after cleavage. In *E. coli*, and most certainly in staphylococci as well, the processivity of the major exonucleases RecBCD and RecJ can be as high as 1 kb per second (Lovett and Kolodner, 1989; Roman et al., 1992). At this rate of degradation, the nicked and/or linear forms of a small plasmid such as pTarget (4.6 kb) will be completely degraded in a few seconds and will not be detected by ethidium bromide staining of plasmids subjected to agarose gel electrophoresis. Alternatively, the Cas10-Csm complex itself could degrade the target DNA. Supporting this hypothesis, our results show that at longer incubation times the substrate's signal disappears (Figure 1E). Indeed, purified *S. epidermidis* Cas10 has been shown to harbor ssDNA exonucleolytic activity, although not in the context of the Cas10-Csm complex (Rama et al., 2014). It is possible that this exonuclease activity is faster in vivo than in vitro and could be potentially responsible for the rapid degradation of the target plasmid in vivo.

Two recent studies showed the crRNA-guided RNA cleavage of the type III-A CRISPR-Cas systems of *S. thermophilus* and *T. thermophilus* (Staals et al., 2014; Tamulaitis et al., 2014). Here, we corroborated these results, and in addition we showed that this RNase activity (1) is responsible for the cleavage of target transcripts during in vivo type III-A CRISPR immunity and (2) is not required for DNA cleavage. In vitro, cleavage is performed by Csm3 within the Cas10-Csm complex and occurs at 6-nt intervals, each cut most likely executed by each of the multiple Csm3 subunits present in the complex. In vivo, primer extension detects only one cleavage, within the crRNA:transcript pairing region. We speculate that this is either due to the impossibility to extend beyond the cut site or to a lower sensitivity of the primer extension assay, which may be allowing us to visualize only the most abundant cleavage products. Alternatively, cellular RNases could degrade the longer cleavage products in vivo, but not in vitro. Also, we detected different cleavage sites in the anti-tag RNA target in vitro and in vivo. In vitro, the cleavage pattern is similar to that the *nes* RNA target, whereas in vivo the extension product is approximately 10 nt shorter, corresponding to a region downstream of the target transcript, within the tag:anti-tag pairing region. It is possible that, in vivo, the RNA cleavage site is measured from the first nucleotides that form the crRNA:transcript pair (i.e., within the anti-tag region). If so, the cleavage site of the anti-tag target will be further downstream to the wild-type target, although we do not understand why this is not the case in vitro. More importantly, the crRNA-guided RNA cleavage

activity of the Cas10-Csm complex is not required for DNA cleavage in vitro and in vivo. The *S. thermophilus* type III-A CRISPR-Cas system was transplanted into *E. coli* and shown that it can confer crRNA-guided immunity against the MS2 ssRNA phage that attacks this host (Tamulaitis et al., 2014). Together with our results, the picture that emerges is that DNA cleavage protects the host from plasmids and dsDNA viruses, whereas RNA cleavage defends from ssRNA viruses. In this view, transcript cleavage could be an unintended consequence of the type III-A system's versatile nucleic acid targeting capability. Of note, *cas10*^{palm} mutant cells, which are capable of RNA-guided RNA cleavage activity only, display a low level of immunity against phage infection (Figure 6, compare with Δ*spc1* control cells). It is tempting to speculate that CRISPR-mediated phage mRNA degradation could contribute to anti-phage immunity in certain conditions. An immune function for mRNA targeting, if any, remains to be determined.

The first observation of crRNA-guided RNA cleavage was obtained with experiments with the *Pyrococcus furiosus* type III-B CRISPR-Cas system (Hale et al., 2009) and was subsequently corroborated for other homolog systems (Zhang et al., 2012). Type III-B CRISPR-Cas loci encode for a Cas10-Cmr complex, homolog to the Cas10-Csm complex of type III-A systems. Genetic experiments with *Sulfolobus islandicus*, an archaeon that contains two type III-B CRISPR-Cas loci suggest that transcription is required for anti-plasmid immunity (Deng et al., 2013) and that these systems can cleave RNA transcripts derived from anti-tag targets (Peng et al., 2015). Combining these observations for type III-B CRISPR immunity, the conservation between both CRISPR subtypes and our data, we propose a unified molecular mechanism for all type III CRISPR-Cas systems: co-transcriptional crRNA-guided DNA and RNA targeting performed by Cas10-Csm/Cmr complexes. This is in sharp opposition to the type I and II CRISPR-Cas systems that have been studied so far, which rely strictly on DNA sequence recognition (Edgar and Qimron, 2010; Garneau et al., 2010; Jinek et al., 2012; Semenova et al., 2011). The broad-target recognition capabilities of type III CRISPR-Cas systems provide a versatile immune response against many different viruses, plasmids, and other mobile genetic elements that coexist with bacteria and archaea.

EXPERIMENTAL PROCEDURES

Purification of Recombinant Cas10-Csm Complex from *E. coli*

Plasmid pPS22 (Hatoum-Aslan et al., 2013) was used to express the Cas10-Csm complex in *E. coli*. To generate the *csm3*^{D32A} mutation (in plasmid pPS086) pPS22 was used as template for PCR with two set of primers PS153/PS465 and PS154/PS466 (the sequences of all oligonucleotides used in this study are in Table S1), and the products were joined by Gibson assembly (Gibson et al., 2009). Full sequencing of the cloned DNA fragments was performed to corroborate the presence of the mutation. The *cas10*$^{D586A-D587A}$ mutation (in plasmid pPS096) was generated in a similar way using the sets of primers PS556/PS559 and PS557/PS558.The wild-type and mutant Cas10-Csm protein complexes were purified as previously described (Hatoum-Aslan et al., 2013) with minor modifications (see Supplemental Experimental Procedures).

Oligonucleotide Substrates

DNA and RNA oligonucleotides were purchased from IDT. They were radiolabeled at the 5′ end with T4 polynucleotide kinase (NEB) and γ-^{32}P ATP (PerkinElmer) in a 1 × T4 polynucleotide kinase buffer at 37°C for 1 hr in a 50-μl reaction. The ssDNA and ssRNA substrates were subjected to denaturing gel purification. The oligonucleotide bands were visualized by autoradiography and excised, eluted into 1 M ammonium acetate (pH 8), 0.2% SDS, and 20 mM EDTA at 4°C overnight, ethanol precipitated, and resuspended in 10 mM Tris-HCl (pH 8) (for DNA) (pH 6.8) (for RNA), 1 mM EDTA. To generate dsDNA substrates T4 PNK was first heat inactivated (at 65°C for 20 min), and then the reactions were purified using an Illustra Microspin G50 column (GE Healthcare) to remove excess γ-^{32}P ATP. Duplex substrates were generated by heating annealing labeled oligonucleotides with twice-molar excess of unlabeled complementary oligonucleotides in the annealing buffer (20 mM Tris-Cl [pH 7.5], 100 mM KCl, 5 mM $MgCl_2$, and 5% glycerol) at 90°C for 10 min, followed by slow cooling to room temperature. Duplexes were separated from single-stranded DNA by 6% native PAGE conducted at 4°C. The duplex bands were visualized by autoradiography and excised, eluted into 10 mM Tris-HCl (pH 8), 1 mM EDTA at 4°C overnight, ethanol precipitated, and resuspended in 10 mM Tris-HCl (pH 8), 1 mM EDTA. The sequences of DNA and RNA oligonucleotides used in this study are listed in Tables S1 and S2, respectively.

Transcription Coupled DNA Cleavage

Elongation complexes (ECs) were reconstituted essentially as described in Sidorenkov et al. (1998). Typically, 2 μl 1 pmol/μl of template strand (TS) and 1 μl of 4 pmol/μl RNA oligos were mixed in 1 × transcription buffer and incubated at 65°C for 5 min, followed by gradual cooling to room temperature. After addition of 1.5 μl *E. coli* RNAP core enzyme (NEB), the reaction was incubated at 25°C for 25–30 min and at 37°C for 1 min. Then, 4 μl 1.25 pmol/μl nontemplate strand (NTS) (pretreated by heating to 65°C for 5 min, then on ice for 2 min, and finally at 37°C for 2 min) was added and incubated for 10–15 min at 37°C. The final concentration of TS was 0.10 pmol/μl after adding supplement buffer to obtain transcription conditions. Assembled ECs were kept on ice until use. In a transcription coupled DNA cleavage assay, Cas10-Csm complex was added to a final concentration of 15 ng/μl. Transcription was initiated with the addition of 2.5 mM of RNTPs. All the reactions were performed at 37°C. For the elongation complex with labeled RNA primer, Cas10-Csm and RNTPs were added to the elongation complex in two different orders. In lanes indicated by (a), the Cas10-Csm complex was added to the elongation complex (EC) and incubated for 10 min; prior to the addition of RNTPs. In lanes indicated by (b), RNTPs were added to the elongation complex and the reaction was incubated for 10 min, followed by the addition of the Cas10-Csm complex. For all the DNA cleavage time course experiments, RNTPs were added to the elongation complex (EC), prior to the addition of Cas10-Csm complex. After addition of Cas10-Csm, the samples were collected at timed intervals of 30 min, 1 hr, 1 hr 30 min, and 2 hr and quenched by mixing with Proteinase K (NEB) and 20 mM EDTA. The DNA/RNA samples were then extracted using phenol-chloroform-isoamyl alcohol (25:24:1), ethanol precipitated and resuspended into loading buffer (90% formamide). The DNA products were heater at 95°C for 5 min before loading onto the gel. Cleavage products were resolved on a 12% denaturing polyacrylamide gels containing 7 M urea and visualized by phosphorimaging (Typhoon, GE Life Sciences).

RNA Cleavage

RNA cleavage reactions were performed at 37°C with 0.1 pmol of 5′-radiolabeled RNA and 100 ng of Cas10-Csm complex in the reaction buffer (25 mM Tris-HCl [pH 7.5], 10 mM $MgCl_2$, 2 mM TCEP). Reactions were initiated by addition of the Cas10/Csm complex. The samples were collected at timed intervals and quenched by mixing 10 μl of reaction mixture with 2 × loading buffer (90% formamide, 50 mM EDTA). The reaction products were separated on a 14% denaturing PAGE and visualized by phosphorimaging (Typhoon, GE Life Sciences). ^{32}P-5′-labeled RNA Decade marker (Ambion) was used as a size marker. To map the cleavage products, oligoribonucleotide markers were generated by RNase A (Life Technologies), RNase T1 (Life Technologies) treatment of RNA substrates for 10 min at 22°C, or by alkaline hydrolysis in 50 mM $NaHCO_3$ (pH 9.5) at 95°C for 10 min.

Transformation

Cultivation of *S. aureus* RN4220 (Kreiswirth et al., 1983), was carried out in tryptic soy (TS) broth at 37°C. Whenever applicable, media were

supplemented with chloramphenicol at 10 μg/ml or erythromycin at 5 μg/ml to ensure pC194- (Horinouchi and Weisblum, 1982a) (pCRISPR) and pE194-derived (Horinouchi and Weisblum, 1982b) (pTarget) plasmid maintenance, respectively. Transformations were performed as previously described (Goldberg et al., 2014) using 100 μl of competent cells and 500 μg of plasmid DNA. After electroporation transformants were plated on TS agar plates containing chloramphenicol and erythromycin for the selection of pCRISPR and pTarget derivatives, respectively, with or without anhydrotetracycline (aTc). Plates without aTc were incubated at 37°C for 12 hr and plates with aTc at 37°C for 36 hr before counting colony-forming units. Construction of plasmid pCRISPR and its *cas10*^{palm} derivative was described previously (Hatoum-Aslan et al., 2013). The *csm3*^{D32A} mutation was introduced into pCRISPR using pPS22 as template for two PCRs with two set of primers PS153/PS465 and PS154/PS466; the products were joined by Gibson assembly to generate pPS87. pTarget construction was reported previously (Goldberg et al., 2014) as pWJ153. Its pTarget$^{anti\text{-}tag}$ derivative was generated by Gibson assembly of a PCR product obtained using pWJ153 as template and primers NP36 and NP37.

Inducible CRISPR Immunity

The experiment was performed as previously described (Goldberg et al., 2014), with the following modifications. Overnight cultures were started from a single transformant colony obtained in the absence of aTc, grown in 3 ml of TS broth supplemented with chloramphenicol and erythromycin. Cultures are diluted to an OD_{600} ~0.1 OD in 5ml TSB with only chloramphenicol and grown for 1 hr. At this point (time zero in the assay) CRISPR targeting is induced by adding aTc to a final concentration of 0.25 μg/ml. Cells were collected at different times after induction and either plasmid DNA or total RNA was purified using a minprep kit (QIAGEN) or TRIzol (Life Technologies), respectively. Primer extension assays were performed as reported elsewhere (Hatoum-Aslan et al., 2011) using primers A248 and A67 for the detection of target cleavage and 5S rRNA, respectively.

Phage Infections

Infection of *S. aureus* RN4220 cells with bacteriophage ΦNM1γ6 was performed as described previously (Goldberg et al., 2014). The spacer targeting the *gp43* gene of the phage was introduced by phosphorylating and annealing the oligonucleotides oGG250 and oGG251 and ligating them into the pGG-BsaI-R vector digested with BsaI, generating pWJ191 (wild-type type III-A pCRISPR plasmid in Figure 6B). pGG-BsaI-R was used as the no-spacer control (Δ*spc1*). This vector was derived from pGG3-BsaI (Goldberg et al., 2014) via two consecutive steps of 'round-the-horn PCR (Moore et al., 2008) followed by blunt ligation. First, spacer 1 was removed from pGG3-BsaI to create pGG-BsaI, using primers oGG164 and oGG165. Second, a downstream repeat was added using primers W845 and W846 to create pGG-BsaI-R. The *cas10*^{palm} derivative was constructed by Gibson assembly of two PCR products: one using primers W494 and W1020 and pLM547 (Hatoum-Aslan et al., 2013) as template, and another using primers W1021 and W1022 and pWJ191 as template. The *csm3*^{D32A} mutation was introduced into pCRISPR using pWJ191 as template for two PCRs with two set of primers PS153/PS465 and PS154/PS466; the products were joined by Gibson assembly to generate pPS87. Construction of the plasmid harboring the type II-A CRISPR-Cas system of *S. pyogenes* targeting the gp43 gene (pGG37) was described elsewhere (Goldberg et al., 2014).

SUPPLEMENTAL INFORMATION

Supplemental Information includes Supplemental Experimental Procedures, three figures, and two tables and can be found with this article online at http://dx.doi.org/10.1016/j.cell.2015.04.027.

AUTHOR CONTRIBUTIONS

P.S. designed and performed all biochemical experiments with the Cas10-Csm complex. N.P. and W.J. contributed equally to this work. N.P. collected data on anti-plasmid immunity in vivo. W.J. tested anti-phage immunity of different CRISPR-Cas mutants. N.P., W.J., and G.W.G. constructed the plasmids used in the in vivo experiments. A.H.-A. designed and assisted with primer extension analysis. L.A.M. and P.S. wrote the manuscript.

ACKNOWLEDGMENTS

We are grateful to Seth Darst, Arkady Mustaev, and Brian Bae for providing CBR703 and help with transcription inhibition assays. We also like to thank Andrew Varble for critical reading of the manuscript. P.S. is supported by a Helmsley Postdoctoral Fellowship for Basic and Translational Research on Disorders of the Digestive System at The Rockefeller University. L.A.M. is supported by the Searle Scholars Program, Rita Allen Scholars Program, an Irma T. Hirschl Award, a Sinsheimer Foundation Award and a NIH Director's New Innovator Award (1DP2AI104556-01).

Received: January 6, 2015
Revised: March 31, 2015
Accepted: April 7, 2015
Published: May 7, 2015

REFERENCES

Anantharaman, V., Iyer, L.M., and Aravind, L. (2010). Presence of a classical RRM-fold palm domain in Thg1-type 3′- 5′nucleic acid polymerases and the origin of the GGDEF and CRISPR polymerase domains. Biol. Direct *5*, 43.

Artsimovitch, I., Chu, C., Lynch, A.S., and Landick, R. (2003). A new class of bacterial RNA polymerase inhibitor affects nucleotide addition. Science *302*, 650–654.

Barrangou, R., and Marraffini, L.A. (2014). CRISPR-Cas systems: Prokaryotes upgrade to adaptive immunity. Mol. Cell *54*, 234–244.

Barrangou, R., Fremaux, C., Deveau, H., Richards, M., Boyaval, P., Moineau, S., Romero, D.A., and Horvath, P. (2007). CRISPR provides acquired resistance against viruses in prokaryotes. Science *315*, 1709–1712.

Bolotin, A., Quinquis, B., Sorokin, A., and Ehrlich, S.D. (2005). Clustered regularly interspaced short palindrome repeats (CRISPRs) have spacers of extrachromosomal origin. Microbiology *151*, 2551–2561.

Brouns, S.J., Jore, M.M., Lundgren, M., Westra, E.R., Slijkhuis, R.J., Snijders, A.P., Dickman, M.J., Makarova, K.S., Koonin, E.V., and van der Oost, J. (2008). Small CRISPR RNAs guide antiviral defense in prokaryotes. Science *321*, 960–964.

Carte, J., Wang, R., Li, H., Terns, R.M., and Terns, M.P. (2008). Cas6 is an endoribonuclease that generates guide RNAs for invader defense in prokaryotes. Genes Dev. *22*, 3489–3496.

Deng, L., Garrett, R.A., Shah, S.A., Peng, X., and She, Q. (2013). A novel interference mechanism by a type IIIB CRISPR-Cmr module in *Sulfolobus*. Mol. Microbiol. *87*, 1088–1099.

Deveau, H., Barrangou, R., Garneau, J.E., Labonté, J., Fremaux, C., Boyaval, P., Romero, D.A., Horvath, P., and Moineau, S. (2008). Phage response to CRISPR-encoded resistance in *Streptococcus thermophilus*. J. Bacteriol. *190*, 1390–1400.

Edgar, R., and Qimron, U. (2010). The Escherichia coli CRISPR system protects from λ lysogenization, lysogens, and prophage induction. J. Bacteriol. *192*, 6291–6294.

Garneau, J.E., Dupuis, M.E., Villion, M., Romero, D.A., Barrangou, R., Boyaval, P., Fremaux, C., Horvath, P., Magadán, A.H., and Moineau, S. (2010). The CRISPR/Cas bacterial immune system cleaves bacteriophage and plasmid DNA. Nature *468*, 67–71.

Gibson, D.G., Young, L., Chuang, R.Y., Venter, J.C., Hutchison, C.A., 3rd, and Smith, H.O. (2009). Enzymatic assembly of DNA molecules up to several hundred kilobases. Nat. Methods *6*, 343–345.

Goldberg, G.W., Jiang, W., Bikard, D., and Marraffini, L.A. (2014). Conditional tolerance of temperate phages via transcription-dependent CRISPR-Cas targeting. Nature *514*, 633–637.

Hale, C.R., Zhao, P., Olson, S., Duff, M.O., Graveley, B.R., Wells, L., Terns, R.M., and Terns, M.P. (2009). RNA-guided RNA cleavage by a CRISPR RNA-Cas protein complex. Cell *139*, 945–956.

Hatoum-Aslan, A., Maniv, I., and Marraffini, L.A. (2011). Mature clustered, regularly interspaced, short palindromic repeats RNA (crRNA) length is measured by a ruler mechanism anchored at the precursor processing site. Proc. Natl. Acad. Sci. USA *108*, 21218–21222.

Hatoum-Aslan, A., Samai, P., Maniv, I., Jiang, W., and Marraffini, L.A. (2013). A ruler protein in a complex for antiviral defense determines the length of small interfering CRISPR RNAs. J. Biol. Chem. *288*, 27888–27897.

Hatoum-Aslan, A., Maniv, I., Samai, P., and Marraffini, L.A. (2014). Genetic characterization of antiplasmid immunity through a type III-A CRISPR-Cas system. J. Bacteriol. *196*, 310–317.

Heitman, J., Ivanenko, T., and Kiss, A. (1999). DNA nicks inflicted by restriction endonucleases are repaired by a RecA- and RecB-dependent pathway in *Escherichia coli*. Mol. Microbiol. *33*, 1141–1151.

Horinouchi, S., and Weisblum, B. (1982a). Nucleotide sequence and functional map of pC194, a plasmid that specifies inducible chloramphenicol resistance. J. Bacteriol. *150*, 815–825.

Horinouchi, S., and Weisblum, B. (1982b). Nucleotide sequence and functional map of pE194, a plasmid that specifies inducible resistance to macrolide, lincosamide, and streptogramin type B antibodies. J. Bacteriol. *150*, 804–814.

Jinek, M., Chylinski, K., Fonfara, I., Hauer, M., Doudna, J.A., and Charpentier, E. (2012). A programmable dual-RNA-guided DNA endonuclease in adaptive bacterial immunity. Science *337*, 816–821.

Kreiswirth, B.N., Löfdahl, S., Betley, M.J., O'Reilly, M., Schlievert, P.M., Bergdoll, M.S., and Novick, R.P. (1983). The toxic shock syndrome exotoxin structural gene is not detectably transmitted by a prophage. Nature *305*, 709–712.

Lovett, S.T., and Kolodner, R.D. (1989). Identification and purification of a single-stranded-DNA-specific exonuclease encoded by the recJ gene of Escherichia coli. Proc. Natl. Acad. Sci. USA *86*, 2627–2631.

Makarova, K.S., Aravind, L., Wolf, Y.I., and Koonin, E.V. (2011a). Unification of Cas protein families and a simple scenario for the origin and evolution of CRISPR-Cas systems. Biol. Direct *6*, 38.

Makarova, K.S., Haft, D.H., Barrangou, R., Brouns, S.J., Charpentier, E., Horvath, P., Moineau, S., Mojica, F.J., Wolf, Y.I., Yakunin, A.F., et al. (2011b). Evolution and classification of the CRISPR-Cas systems. Nat. Rev. Microbiol. *9*, 467–477.

Marraffini, L.A., and Sontheimer, E.J. (2008). CRISPR interference limits horizontal gene transfer in staphylococci by targeting DNA. Science *322*, 1843–1845.

Marraffini, L.A., and Sontheimer, E.J. (2010). Self versus non-self discrimination during CRISPR RNA-directed immunity. Nature *463*, 568–571.

Mojica, F.J., Díez-Villaseñor, C., García-Martínez, J., and Soria, E. (2005). Intervening sequences of regularly spaced prokaryotic repeats derive from foreign genetic elements. J. Mol. Evol. *60*, 174–182.

Mojica, F.J., Díez-Villaseñor, C., García-Martínez, J., and Almendros, C. (2009). Short motif sequences determine the targets of the prokaryotic CRISPR defence system. Microbiology *155*, 733–740.

Moore, M.R., Gertz, R.E., Jr., Woodbury, R.L., Barkocy-Gallagher, G.A., Schaffner, W., Lexau, C., Gershman, K., Reingold, A., Farley, M., Harrison, L.H., et al. (2008). Population snapshot of emergent *Streptococcus pneumoniae* serotype 19A in the United States, 2005. J. Infect. Dis. *197*, 1016–1027.

Peng, W., Feng, M., Feng, X., Liang, Y.X., and She, Q. (2015). An archaeal CRISPR type III-B system exhibiting distinctive RNA targeting features and mediating dual RNA and DNA interference. Nucleic Acids Res. *43*, 406–417.

Pourcel, C., Salvignol, G., and Vergnaud, G. (2005). CRISPR elements in *Yersinia pestis* acquire new repeats by preferential uptake of bacteriophage DNA, and provide additional tools for evolutionary studies. Microbiology *151*, 653–663.

Ramia, N.F., Tang, L., Cocozaki, A.I., and Li, H. (2014). *Staphylococcus epidermidis* Csm1 is a 3′-5′ exonuclease. Nucleic Acids Res. *42*, 1129–1138.

Roman, L.J., Eggleston, A.K., and Kowalczykowski, S.C. (1992). Processivity of the DNA helicase activity of Escherichia coli recBCD enzyme. J. Biol. Chem. *267*, 4207–4214.

Semenova, E., Jore, M.M., Datsenko, K.A., Semenova, A., Westra, E.R., Wanner, B., van der Oost, J., Brouns, S.J., and Severinov, K. (2011). Interference by clustered regularly interspaced short palindromic repeat (CRISPR) RNA is governed by a seed sequence. Proc. Natl. Acad. Sci. USA *108*, 10098–10103.

Sidorenkov, I., Komissarova, N., and Kashlev, M. (1998). Crucial role of the RNA:DNA hybrid in the processivity of transcription. Mol. Cell *2*, 55–64.

Staals, R.H., Zhu, Y., Taylor, D.W., Kornfeld, J.E., Sharma, K., Barendregt, A., Koehorst, J.J., Vlot, M., Neupane, N., Varossieau, K., et al. (2014). RNA targeting by the type III-A CRISPR-Cas Csm complex of *Thermus thermophilus*. Mol. Cell *56*, 518–530.

Tamulaitis, G., Kazlauskiene, M., Manakova, E., Venclovas, Č., Nwokeoji, A.O., Dickman, M.J., Horvath, P., and Siksnys, V. (2014). Programmable RNA shredding by the type III-A CRISPR-Cas system of *Streptococcus thermophilus*. Mol. Cell *56*, 506–517.

van der Oost, J., Westra, E.R., Jackson, R.N., and Wiedenheft, B. (2014). Unravelling the structural and mechanistic basis of CRISPR-Cas systems. Nat. Rev. Microbiol. *12*, 479–492.

Westra, E.R., van Erp, P.B., Künne, T., Wong, S.P., Staals, R.H., Seegers, C.L., Bollen, S., Jore, M.M., Semenova, E., Severinov, K., et al. (2012). CRISPR immunity relies on the consecutive binding and degradation of negatively supercoiled invader DNA by Cascade and Cas3. Mol. Cell *46*, 595–605.

Zhang, J., Rouillon, C., Kerou, M., Reeks, J., Brugger, K., Graham, S., Reimann, J., Cannone, G., Liu, H., Albers, S.V., et al. (2012). Structure and mechanism of the CMR complex for CRISPR-mediated antiviral immunity. Mol. Cell *45*, 303–313.